PCASP Measurements and Data Processing (Version 2: 20190628)

Jeff Snider
Shelby Fuller
Matt Burkhart

University of Wyoming
Department of Atmospheric Science
Laramie, WY

1 – Introduction

This document reports on processing of data from a Passive Cavity Aerosol Spectrometer Probe (PCASP). There are five objectives: 1) To report on calibrations of the PCASP flow system. 2) Using two refractive index formulations, to report on PCASP sizing of aerosol particles. The refractive index formulations are 1.59 + 0.00·i (polystyrene latex) and 1.50 + 0.04·i (wildfire smoke aerosol). 3) To develop a computer algorithm that estimates bias in PCASP data due to particle coincidence within the instrument's sample volume. This bias is significant in environments with unusually large aerosol number concentrations ($N > 5000$ cm^{-3}; $D > 0.1$ µm) (e.g., within wildfire smoke plumes). 4) To estimate coincidence-induced bias in PCASP-derived values of aerosol volume. 5) To apply the bias correction to PCASP data acquired in a wildfire smoke plume.

Two PCASPs were flown on the King Air during 2018 and 2019. As in Cai et al. (2013), we refer to these as PCASP-1 and PCASP-2. Both are equipped with the SPP200 electronic package developed by Droplet Measurements Technologies (DMT 2000). During the BBFLUX project, PCASP-2 was flown between 20180721 to 20180812, and PCASP-1 was flown between 20180819 to 20180917. After BBFLUX, both PCASP-1 and PCASP-2 were flown on the King Air on 20180928. The PCASP-1 was flown on the King Air during the TECPEC project (20190301 to 20190331).

2 - Flow Calibration

The PCASP's flow system is shown in Figure 1. The sample flow systems of PCASP-1 and PCASP-2 were calibrated May 2018, August 2018, and April 2019 (Figures 2 and 3). The curves labeled "ALL" are the calibrations recommended for data acquired during BBFLUX, TECPEC, and on 20180928. In these plots, Q_{sample} is the sample flow rate (standard cubic centimeter per second), and V_{out} is the output voltage of the sample flow sensor (Volt).

Equations 1a – b represent the sheath flow calibrations.

$$Q_{sheath} = 0.604 \cdot \exp\left(0.675 \cdot V_{out}\right) \quad \text{(PCASP-1)} \quad (1a)$$

$$Q_{sheath} = 0.583 \cdot \exp\left(0.651 \cdot V_{out}\right) \quad \text{(PCASP-2)} \quad (1b)$$

In these equations Q_{sheath} is the sheath flowrate (standard cubic centimeter per second) and V_{out} is the output voltage of the sheath flow sensor (Volt). All flow calibrations were done in the Keck Aerosol Laboratory at the University of Wyoming.

3 – Particle Sizing Calibration

Polystyrene latex (PSL) particles were used in May 2018 and in August 2018 to calibrate particle sizing by PCASP-1 and PCASP-2. These calibrations were done in the Keck Aerosol Laboratory at the University of Wyoming. In general, the manufacturer's recommendation for the relationship between particle size and scattered light intensity (threshold) was adhered to. Table 2 presents the manufacturer's relationship. Additionally, laboratory calibrations were conducted in April 2019. These indicate a 20% low bias in sizing by PCASP-1. Since it is not known when this sizing bias occurred, its effect on BBFLUX measurements was not evaluated.

Table 3 has an approximate relationship for particle size and threshold for wildfire smoke aerosol. In Snider and Burkhart (2019), we used four refractive formulations (1.90 + 0.01·i, 1.90 + 0.04·i, 1.50 + 0.01·i, and 1.50 + 0.04·i) and demonstrated that the index 1.50 + 0.04·i maximizes aerosol extinction at wavelength equal to 0.5 μm.

4 - Coincidence Bias

Within the PCASP's sample cavity, the sample and sheath streams are combined, cross the laser, and are exhausted into the pump (Fig. 1). Since the laser beam is narrow (~ 0.7 mm), and the speed of the flow stream is ~ 45 m/s (PMS 2002), the interval of time that a particle is transiting the laser is ~ 20 μs.

We are interested in the transit time (τ) because it is a parameter used to correct bias associated with a measured concentration (N_m; D > 0.1 μm). This bias is substantial when N_m is substantially greater than typical for the atmosphere. By typical, we mean N_m ~ 500 cm^{-3}, whereas within smoke plumes N_m ~ 5000 cm^{-3}. It is the occurrence of multiple particles within the PCASP's sample volume which causes the bias. The magnitude of the bias (hereafter, coincidence bias) increases with increasing N_m.

We use Eqn. 2 (Willeke and Liu 1976) to evaluate the coincidence bias.

$$N_C = N_M \exp\left(\tau Q_{sample} N_C\right) \qquad (2)$$

Here N_C is the corrected PCASP concentration.

5 – Transit Time as a Function of Flow Rate

Laboratory measurements conducted using mobility-selected PSL test particles are provided in Table 1. These results demonstrate that the sensitivity of transit time to Q_{sample}, defined as $-\Delta \ln \tau / \Delta \ln Q_{sheath}$, is at least nine times the sensitivity of transit time to Q_{sample} (i.e., $-\Delta \ln \tau / \Delta \ln Q_{sample}$). This result is expected because the sheath flow rate ~ 10 times that of the sample flow rate (PMS 2002). Importantly, these findings indicate that a change of sheath flow can result in a change of transit time, and thus a change of coincidence bias (Eqn. 2), that is independent of sample flow rate.

6 – Analysis of PCASP Data Acquired in a Wildfire Plume

Using data from the King Air flight on 20180928, and Eqn. 2, we evaluated the corrected PCASP number concentration (N_C). Our analysis is based on measurements of τ, Q_{sample}, and N_M. These variables were sampled and recorded at 10 Hz and are available in the "raw" King Air data file (20180928_raw.nc).

We focus on data from the PCASP-1 acquired inside a wildfire plume. The plume is seen in Fig. 4 with the upwind (westerly) portion of the plume on the rhs of the photograph. This photograph was taken at 19:52 UTC, approximately 16 minutes before the King Air encountered plume on a southerly heading. Subsequent to the southerly plume transit, the aircraft turned and transited the plume on a northerly heading. Eight minutes of data (20:07:15 to 20:15:15 UTC), including clean air north of the plume (Fig. 4), the south-heading plume transit, the turn in clean air south of the plume, the north-heading plume transit, and resampling of clean air north of the plume, are analyzed in the following paragraphs.

For each set of measurements (τ, Q_{sample}, and N_M), the unknown in Eqn. 2 is the corrected concentration (N_C). Values of N_C were computed using a nonlinear equation solver (fx_root; Interactive Data Language, Harris Geospatial Solutions, Inc.). Sequences of measurements, and the calculated coincidence correction factor (N_C /N_m), are presented in Fig. 5a – d. Outside of the plume (e.g., early in the time sequence), the correction factor (Fig. 5d) is essentially one, however, within a nine-second segment of the plume, indicated by dashed-vertical lines, the correction factor ~ 1.1 (Fig. 5d).

Fig. 6a – d portray the PCASP concentration size distribution (dN/dlogD; top panels) and the PCASP volume size distribution (dV/dlogD; bottom panels). These distributions were picked from the interval indicated by dashed-vertical lines in Fig. 5a – d. Corrected distributions (Fig. 6c and 6d) were estimated using the following hypothesis: *Coincidence diminishes the particle count in channels equal to or smaller than the dN/dlogD mode and this bias is corrected by multiplying the corresponding dN/dlogD values by the coincidence correction factor*. Application of the hypothesis modestly increases dN/dlogD at the mode diameter and at dN/dlogD values smaller than the mode (cf., Fig. 6a and Fig. 6c). For the data subset analyzed, the correction factor increases the averaged size-integrated concentration from $\langle N_M \rangle$ = 7584 cm^{-3} to $\langle N_C \rangle$ = 7978 cm^{-3} (5 %). Because the size-integrated volume is more strongly weighted by

contributions from particles larger than the dN/dlogD mode, the effect of the correction is smaller for size-integrated aerosol volume (2 %) compared to size integrated aerosol concentration (cf., Fig. 6b and Fig. 6d).

7 – Summary

1) Calibrations of the flow systems of PCASP-1 and PCASP-2 are presented and calibration coefficients are recommended for data recorded between May 2018 and May 2019.

2) Laboratory test data is used to establish that particle transit time is more sensitive to sheath flowrate than sample flowrate.

3) Calibrations of the sizing systems of PCASP-1 and PCASP-2 are also discussed. In general, the manufacturer's recommendation for the relationship between PSL size and scattered light intensity was adhered to between May 2018 and May 2019. Particle sizes corresponding to a refractive index for wildfire smoke aerosol is also provided.

4) Coincidence introduces a negative bias in PCASP-derived particle number concentrations. The coincidence correction factor is ~ 1.1 within a wildfire smoke plume where the measured number concentration was ~ 8000 cm^{-3}.

5) A method was developed for correcting coincidence bias in size distributions of aerosol concentration and in size distributions of aerosol volume.

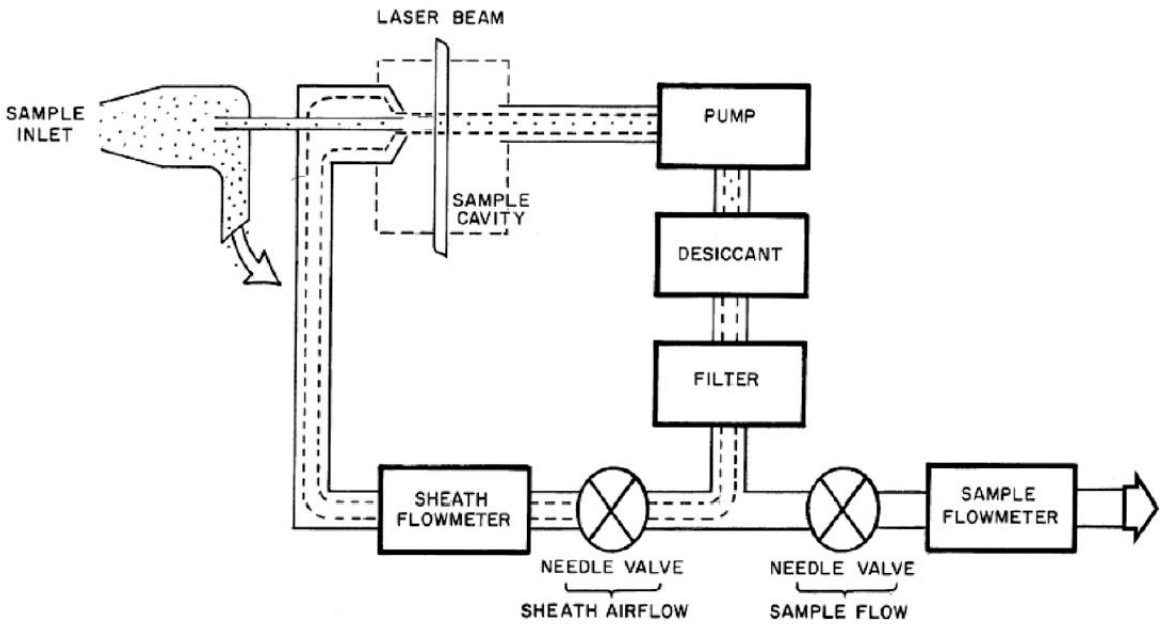

Figure 1 – Flow system of the PCASP (Snider et al. 2017).

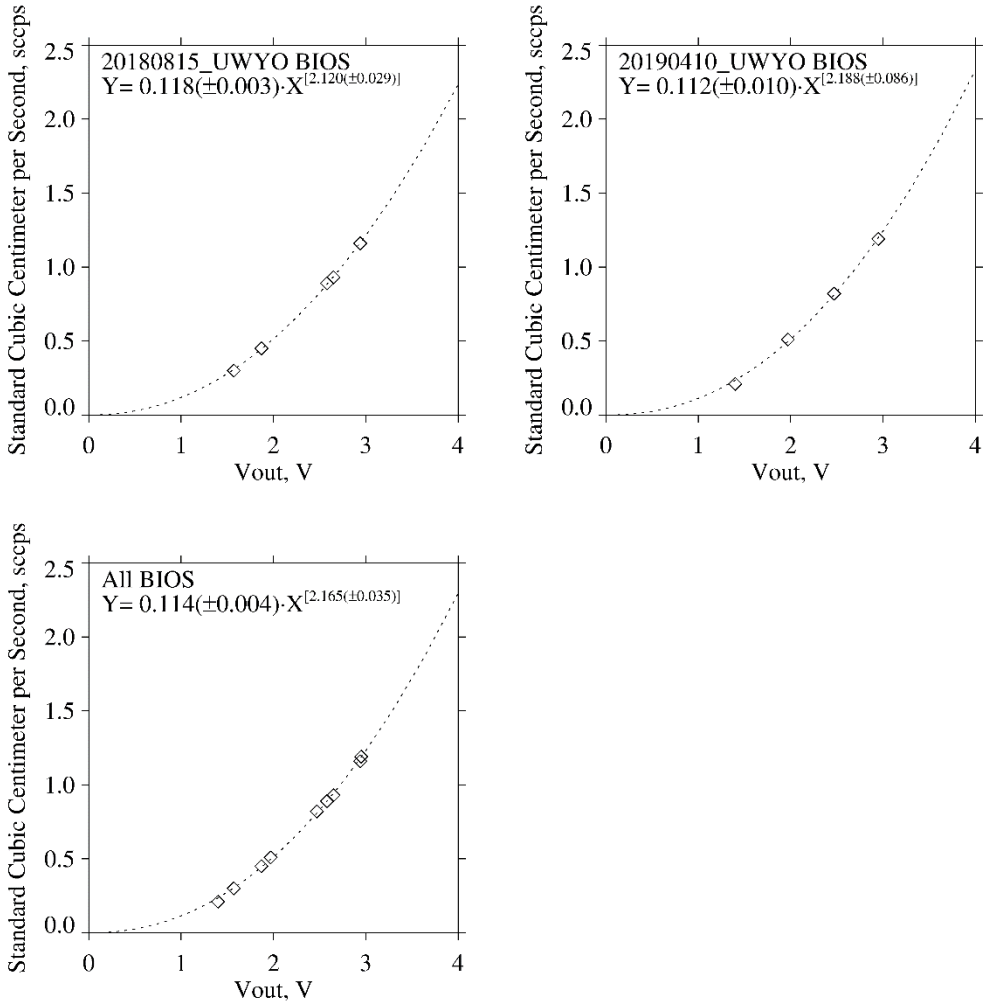

Figure 2 – Calibration of the sample flow system of PCASP-1. The curve labeled “ALL” is the calibration recommended for data acquired during BBFLUX, TECPEC, and on 20180928.

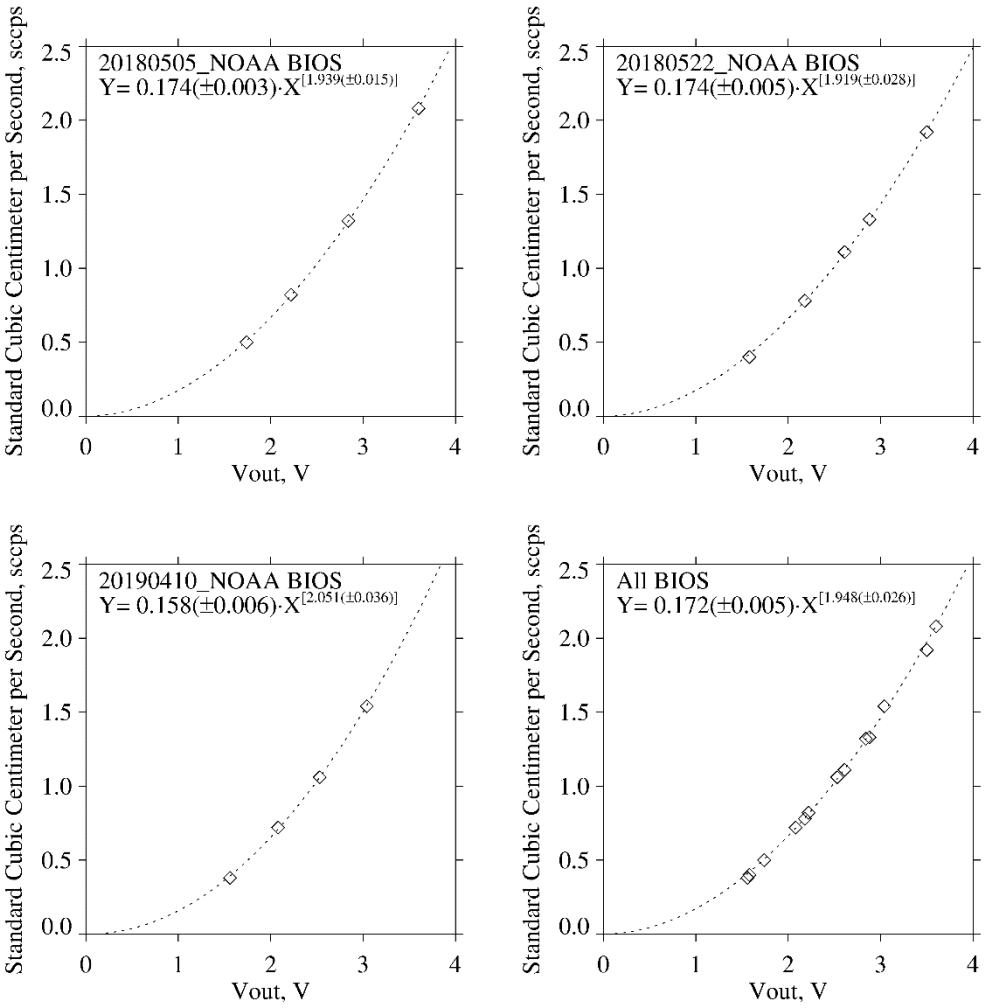

Figure 3 – Calibration of the sample flow system of PCASP-2. The curve labeled "ALL" is the calibration recommended for data acquired during BBFLUX, TECPEC, and on 20180928.

Figure 4 – Photograph of the wildfire plume on 20180928. The King Air is tracking southward. Geographic features in front of the King Air (northward of the plume) are Jelm Mountain (most distant) and Sheep Mountain (closer to the King Air).

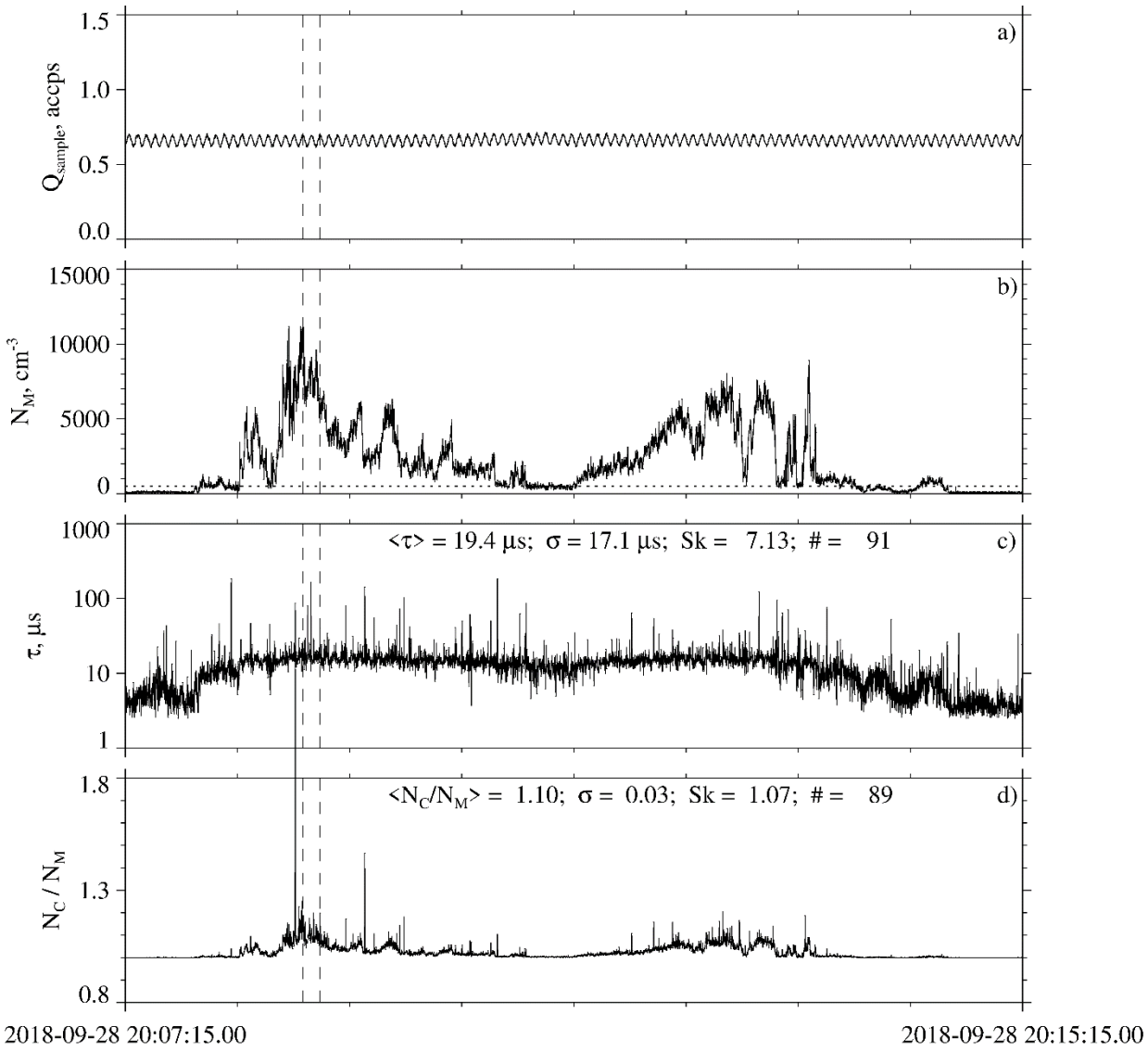

Figure 5 – Data from PCASP-1 on 20180928. a) Sample flow rate. b) Measured concentration with Channel 0 values eliminated. The horizontal dotted line at 500 cm^{-3} is an estimate of the distinction between clean and plume conditions. c) Transit time. d) Coincidence correction factor. Values plotted are 10 Hz samples. Average, standard deviation (σ), and skewness (Sk) in c) and d) are for the 9 s interval indicated by dashed vertical lines.

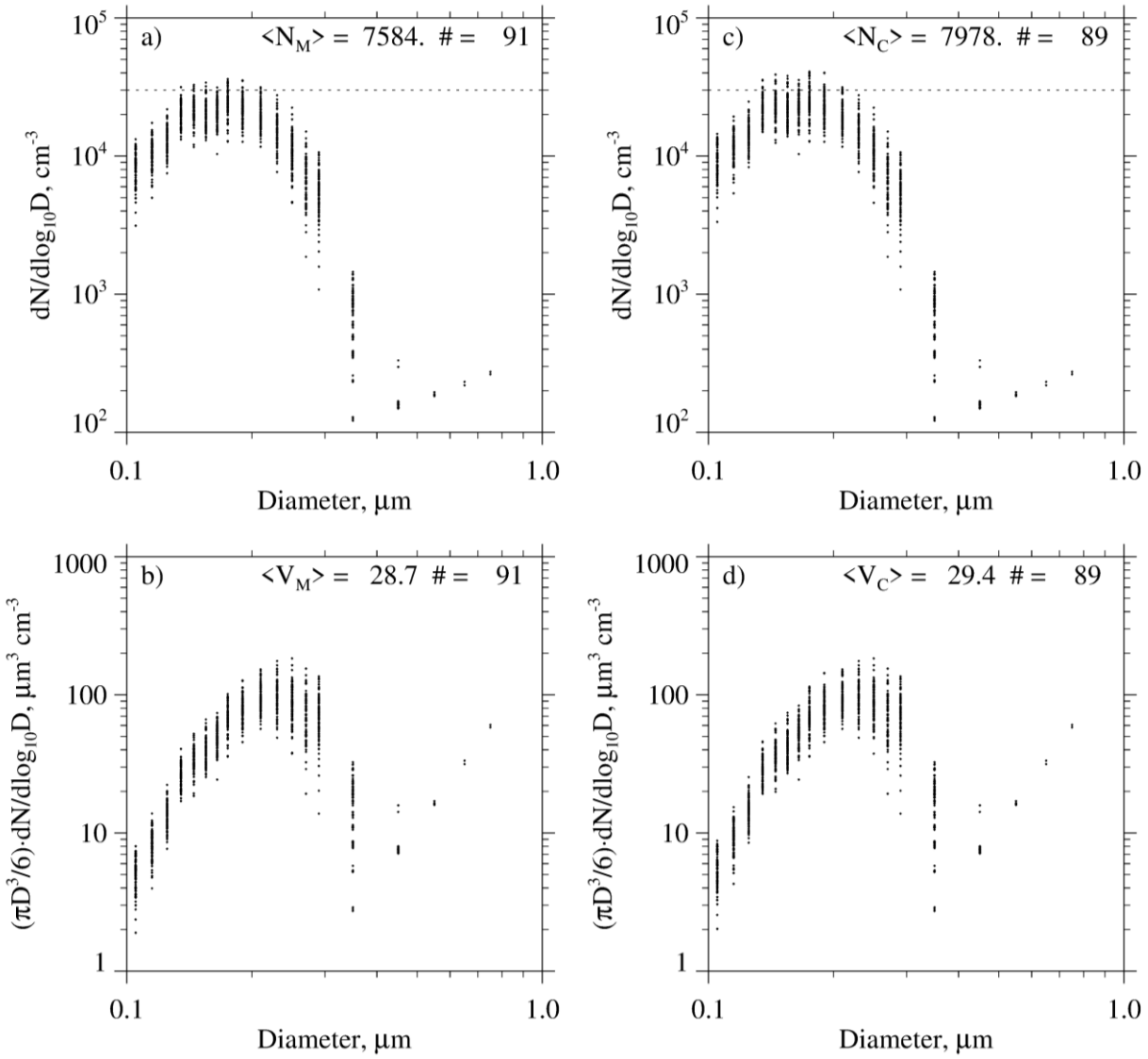

Figure 6 – Data from PCASP-1 on 20180928. a) Concentration size distribution (dN/dlogD vs particle diameter). b) Volume size distribution (dV/dlogD vs particle diameter). c) Concentration size distribution corrected with the hypothesis described in section 7. d) Volume size distribution corrected with the hypothesis described in section 7. Values plotted are 10 Hz samples. Data segment analyzed is indicated with dashed vertical lines in Fig. 5. Channel 0 count values were eliminated from these plots.

Table 1 – Laboratory Measurements [a] of Transit Time, Flowrate, and Calculated Sensitivity

Particle Diameter, nm	Transit Time, µs	Sample Flowrate, sccps [b]	Sheath Flowrate, sccps [b]	Relative Sensitivity (Sample)	Relative Sensitivity (Sheath)
125	7.3	0.77	9.2	0.04 [c]	
125	7.5	0.41	9.4		
125	4.7	0.77	15.0		0.90 [d]
269	15.8	0.88	10.4	0.08 [c]	
269	16.6	0.47	10.8		
269	12.7	0.83	14.4		0.67 [d]
498	19.8	0.81	10.1	0.06 [c]	
498	20.6	0.44	10.6		
498	15.2	0.80	14.8		0.69 [d]
600	21.0	0.83	9.7	0.01 [c]	
600	21.1	0.38	10.1		
600	16.7	0.75	14.8		0.54 [d]

[a] From PCASP-2, recorded 20190503

[b] Standard cubic centimeters per second

[c] Evaluated as $-\Delta \ln \tau / \Delta \ln Q_{sample}$

[d] Evaluated as $-\Delta \ln \tau / \Delta \ln Q_{sheath}$

Table 2 –Polystyrene latex diameters [a] for PCASP-1 and PCASP-2, and Thresholds

Channel Number	Lower-limit Diameter, μm	Upper-limit Diameter, μm	Threshold [b]
0 [c]	0.09	0.10	692
1	0.10	0.11	1146
2	0.11	0.12	1814
3	0.12	0.13	2769
4	0.13	0.14	4096
5	0.14	0.15	4192
6	0.15	0.16	4231
7	0.16	0.17	4282
8	0.17	0.18	4348
9	0.18	0.20	4537
10	0.20	0.22	4825
11	0.22	0.24	5251
12	0.24	0.26	5859
13	0.26	0.28	6703
14	0.28	0.30	8192
15	0.30	0.40	8335
16	0.40	0.50	8435
17	0.50	0.60	8520
18	0.60	0.70	8768
19	0.70	0.80	8981
20	0.80	0.90	9194
21	0.90	1.00	9418
22	1.00	1.20	9579
23	1.20	1.40	9825
24	1.40	1.60	10080
25	1.60	1.80	10460
26	1.80	2.00	10872
27	2.00	2.30	11322
28	2.30	2.60	11759
29	2.60	3.00	12288

[a] Refractive index of PSL is $1.59 + 0.00 \cdot i$ ($\lambda = 0.633$ μm)

[b] Thresholds are internal electronic representations of the channel boundaries. A digitized pulse height is compared to the thresholds to infer the channel a particle is classified into.

[c] Channel 0 (PCASP-1) particle counts are eliminated from all calculations presented in this report.

Table 3 – Wildfire smoke particle diameters [a] for PCASP-1 and PCASP-2, and Thresholds

Channel Number	Lower-limit Diameter, μm	Upper-limit Diameter, μm	Threshold [b]
0	0.09	0.11	692
1	0.11	0.12	1146
2	0.12	0.13	1814
3	0.13	0.14	2769
4	0.14	0.15	4096
5	0.15	0.16	4192
6	0.16	0.17	4231
7	0.17	0.18	4282
8	0.18	0.19	4348
9	0.19	0.21	4537
10	0.21	0.24	4825
11	0.24	0.26	5251
12	0.26	0.28	5859
13	0.28	0.31	6703
14	0.31	0.33	8192
15	0.33	0.52	8335
16	0.52	0.68	8435
17	0.68	0.86	8520
18	0.86	1.02	8768
19	1.02	1.16	8981
20	1.16	2.51	9194
21	2.51	3.03	9418
22	3.03	3.69	9579
23	3.69	5.09	9825
24	5.09	5.10	10080
25	5.10	5.54	10460
26	5.54	6.31	10872
27	6.31	7.46	11322
28	7.46	8.90	11759
29	8.90	10.83	12288

[a] Refractive index = $1.50 + 0.04 \cdot i$ ($\lambda = 0.633$ μm) is assumed; see section 3.

[b] Thresholds are internal electronic representations of the channel boundaries. A digitized pulse height is compared to the thresholds to infer the channel a particle is classified into.

References

Cai, Y., J.R.Snider and P. Wechsler, Calibration of the passive cavity aerosol spectrometer probe for airborne determination of the size distribution, Atmos. Meas. Tech., 6, 2349-2358, doi:10.5194/amt-6-2349-2013, 2013

Droplet Measurement Technologies, *Signal Processing Package for Optical Particle Counters: Model SPP-200 View Particle Display Operations Manual*, DMT Inc., 24 pp., 2000

Particle Measuring Systems, *PMS Model PCASP-100X 0.10–3.0 μm operating manual*, PMS Inc., 45 pp., 2002

Snider, J.R., D.Leon and Z.Wang, Droplet Concentration and Spectral Broadening in Southeast Pacific Stratocumulus, J. Atmos. Sci., 74, 719-749, 2017

Snider, J.R., and M.Burkhart, PCASP-derived Extinctions in Wildfire Smoke during BBFLUX, http://www-das.uwyo.edu/~jsnider/workshop_poster_snider.pdf, WE-CAN Workshop, 2019

Willeke, K. and B.Y.H.Liu, Single particle optical counter: Principle and applications, in *Fine Particles: Aerosol Generation, Measurement, Sampling, and Analysis*, pp. 698 – 729, editor B.Y.H.Liu, Academic Press, New York, 1976